Analysis of WDS 19121+4951 STF 2486 AB Using GAIA DR3 Data and an Updated Astrometric Measure

Richard C. Jaworski

Macquarie University, Sydney, NSW. Australia; richjaw001@gmail.com

Abstract

This paper analyses the nature of STF 2486 AB using GAIA DR3 data and an updated astrometric measure. STF 2486 AB was imaged using the Las Cumbres Observatory (LCO) Global Network of Telescopes. Calibrated images were obtained and analysed using the software AstroImageJ to determine position angle and separation. Using GAIA DR3 data and apparent separation reported in this paper, minimum, mean and maximum physical distance separation was estimated. In addition, the space velocity of the primary and secondary, angle between each of the components space velocity vectors in 3-dimensional space (Nugent metric), relative 3-dimensional space velocity, system escape velocity and binding energy (E_{binding}) were calculated. GAIA DR3 analysis shows that STF 2486 AB exhibits features consistent with a binary star system.

1. Introduction

Located in the Constellation of Cygnus STF 2486 AB is considered to be a binary star system. Most recent studies have provided astrometric data on this pair (Anton 2017; Brabec et al. 2025). The current paper analyses the nature of STF 2486 in light of GAIA DR3 data and an updated astrometric measure.

STF 2486 AB was first measured in 1819.93 when the position angle was 223.2° and the separation was 9.0″ (Struve 1837). The last measure was in 2025.472 when the position angle was 202.4° and the separation was 7.01″ (Schuhmacher, 2025). STF 2486 AB has 2 orbits in the Sixth Catalog of Orbits of Visual Binary Stars (both grade 4), Figures 1a and 1b (Hale 1994; Izmailov, 2019). A more recent orbit for STF 2486 using the Apparent Motion Parameters Method is in the Pulkovo Catalog of Orbits (Romanenko et al. 2025).

Selected GAIA DR3 data for STF 2486 AB is shown in Table 1 (Prusti et. al. 2016; Vallenari et. al. 2023). The Renormalised Unit Weight Error (RUWE) for the primary is 0.993 and 0.978 for the secondary consistent with good single star models.

STF 2486 also has C and D components in the Washington Double Star Catalog. The parallax of the C component is 1.4087 mas (distance = 710pc) and 5.6581 mas (distance = 177 pc) for the D component and thus AC and AD are optical pairs.

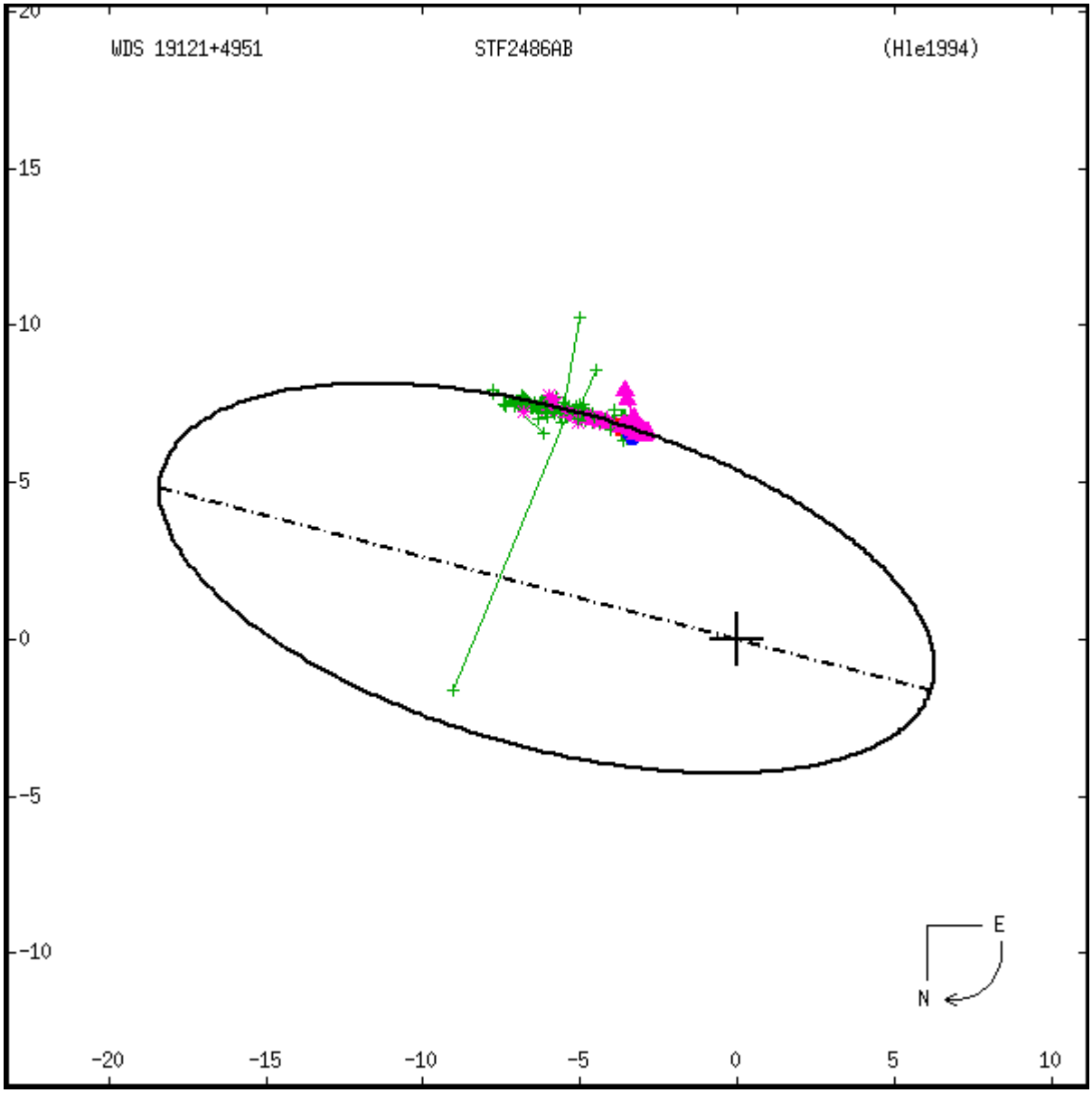

Figure 1a: Apparent orbit of 19121+4951 STF 2486 AB (Hale 1994)

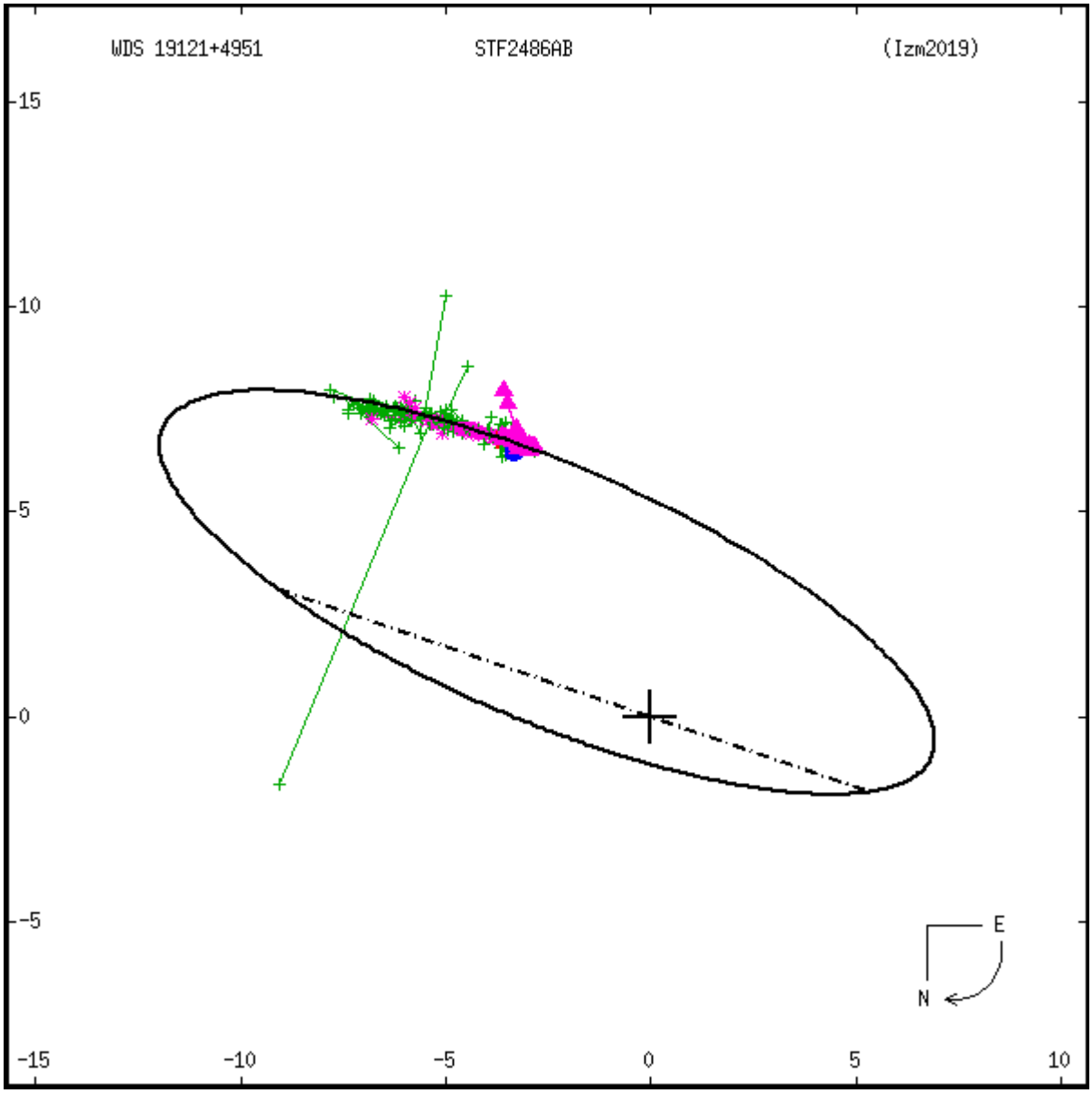

Figure 1b: Apparent orbit of 19121+4951 STF 2486 AB (Izmailov 2019)

Table 1: Selected data on STF 2486 AB from GAIA DR3. Stellar luminosity and mass values come from GAIA DR3 FLAME.

WDS Identifier 19121+4951 STF 2486 AB	**Parallax ± 1σ mas**	**Total proper motion mas/yr**	**pmra ± 1σ mas/yr**	**pmdec ± 1σ mas/yr**	**Radial velocity ± 1σ km/sec**	**Luminosity SolLum**	**Mass $M_\odot$**
A Component Gaia source id: 2132788541955849984	39.5809 ± 0.0157	655.781	-210.538 ± 0.021	621.066 ± 0.019	-41.08 ± 0.18	1.32	0.94
B Component Gaia source id: 2132788541955849216	39.5784 ± 0.0147	656.912	-185.724 ± 0.017	630.111 ± 0.018	-41.82 ± 0.24	1.15	0.92

The distance from the Sun to the primary and secondary of STF 2486 AB with 1σ parallax uncertainties are shown in Figure 2. The distances from the Sun to the primary and secondary show significant overlap.

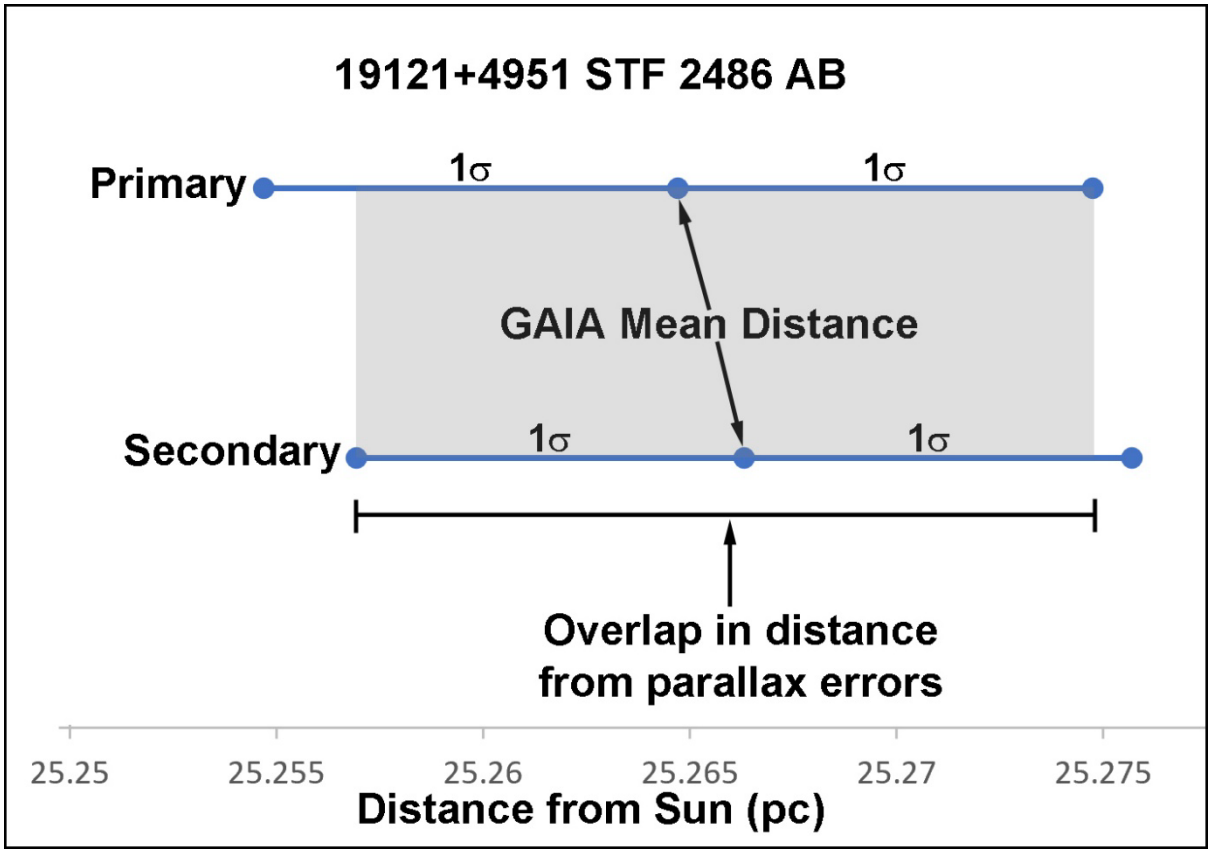

Figure 2: GAIA DR3 distances of the components of STF 2486 AB from the Sun including 1σ parallax errors

2. Methods

Using the Las Cumbres Observatory Global Network of Telescopes, STF 2486 AB was imaged on June 25, 2026 and June 26, 2026 (Mean Decimal Date: 2026.482; Mean JD UTC: 2461217.11) at the LCOGT node at Tenerife, Canary Islands, Spain with a Planewave Delta Rho 350 telescope and QHY600 CMOS camera system. The camera format was 9576 x 6388 pixels, 3.76 micron pixels size. Field of view 1.9 degrees x 1.2 degrees readout mode full-frame, 30'x30' in readout mode central30x30. Pixel size (1x1 binning, arcsec) ~0.74"/pixel, default binning 1 x 1, read noise (e-) ~ 3 to 3.5 e- and gain (e-/ADU) 0.7 e-/ADU.

Twenty images were taken on June 25, 2026 and twenty images were taken on June 26, 2026. The images were recorded through a Bessel-V Filter and the exposure time for each image was 0.5 seconds. The air mass for each image set was 1.1. The image sets were combined and the calibrated images were individually visually inspected for quality and 31 were subsequently chosen for analysis. The images were analysed using AstroImageJ, Figure 3, and mean value, standard deviation and standard error of the mean determined for position angle and separation, Table 2.

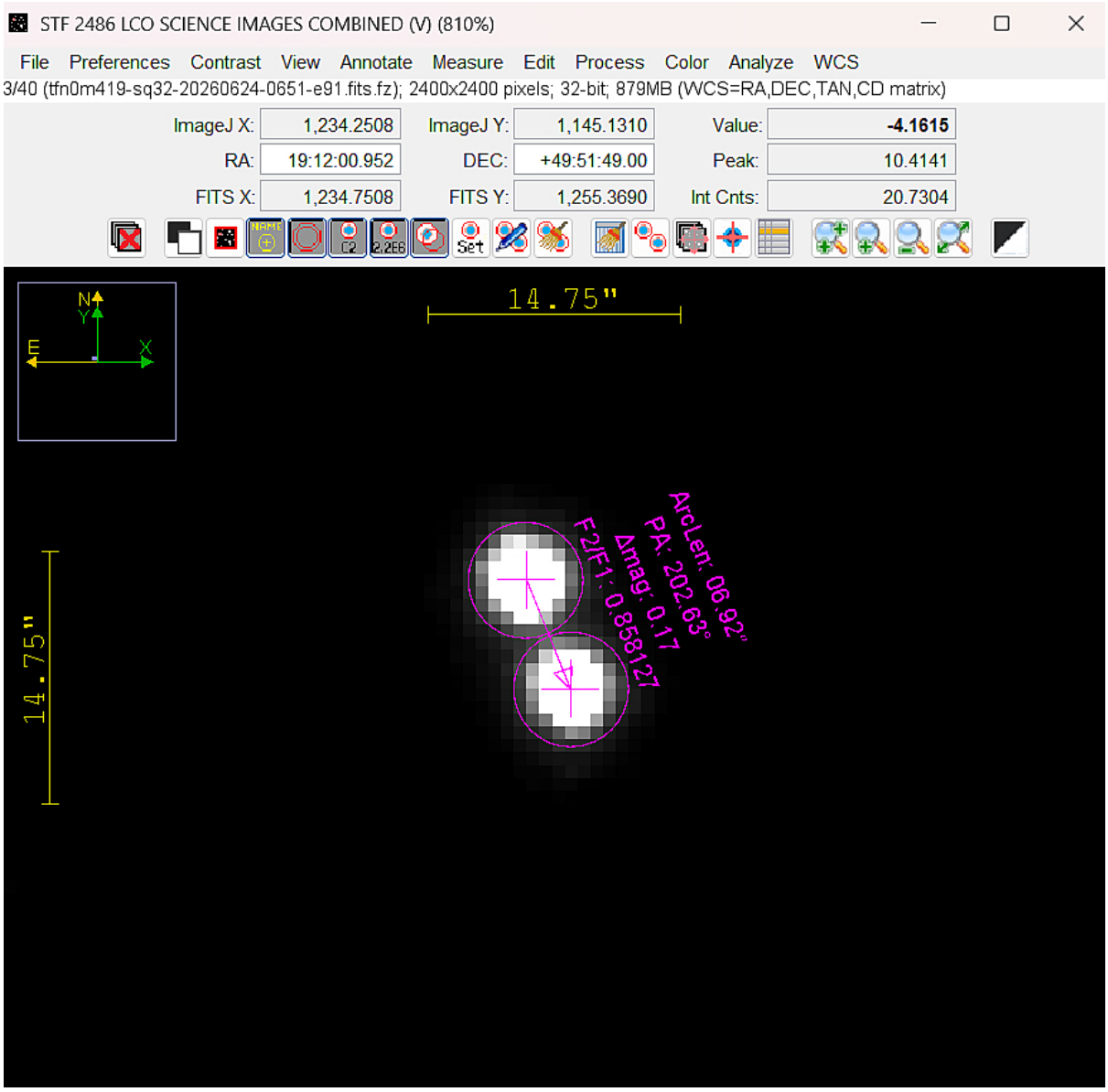

Figure 3: A representative image of STF 2486 AB analysed using AstroImageJ showing separation and position angle.

To calculate D, the mean physical separation distance of the components in pc, the cosine rule was used:

$$D = \sqrt{[D_A^2 + D_B^2 - 2D_A D_B \cos(\rho/3{,}600)]} \quad (1)$$

Where D is the mean separation distance of the two stars in pc; D_A is the mean distance from the Sun to the primary in pc, obtained from parallax measures; D_B is the mean distance from the Sun to the secondary in pc, and ρ is apparent separation in arcseconds (″) reported in this paper, Table 3.

The minimum and maximum distance separation was calculated using the data in Table 1, measure of apparent separation reported in this paper and Equation (1), Table 3.

The angle between each of the components space velocity vectors in 3-dimensions (Nugent metric) was calculated using the method of Nugent (Nugent, 2025), Table 3. Angles < 15° are designated as Common Space Motion pairs, values > 15° and < 30° are designated as Similar Space Motion pairs and values > 30° are designated as Different Space Motion pairs.

The space velocity of the A component and space velocity of the B component was calculated using the method of Nugent (Nugent, 2025). The relative 3-dimensional space velocity and system escape velocity were calculated using the method of Bonifacio (Bonifacio et al, 2020), Table 3.

Binding energy *($E_{binding}$)*, was calculated using the following formula (Letchford et al, 2022).

$$E_{binding} = \frac{1}{2}\left(\frac{m_A m_B}{m_A + m_B}\right) v^2 - \frac{G m_A m_B}{D} \quad (2)$$

Where, $E_{binding}$ is in $M_\odot(\text{km s}^{-1})^2$; m_A and m_B are the masses of the primary and secondary in solar masses ($M_\odot$); v is the galactic space speed difference between the two stars in km s^{-1}; D is their physical separation in parsec (pc); and G is the gravitational constant (4.30091×10^{-3} pc$(\text{km s}^{-1})^2/M_\odot$).

3. Data

The results of the analysis of the 31 images by AstroImageJ are given in Table 2.

Table 2: Position angle and separation determined for STF 2486 AB using AstroImageJ.

Epoch	Measurement (n = 31 images)	Position Angle (degrees)	Separation (arcseconds)
Mean DD: 2026.482 Mean JD: 2461217.110	Mean	202.5	6.97
	Standard Deviation	0.41	0.062
	Standard Error of the Mean	0.07	0.011
Ephemeris*			
2026.0		202.5	6.998
2027.0		202.3	6.979

* Izmailov 2019, Sixth Catalog of Obits of Visual Binary Stars (Matson et al. 2026)

The mean physical distance separation of the primary and secondary of STF 2486 AB is 0.0018 pc which equates to 371 AU.

The binding energy of STF 2486 AB using the mean physical distance separation is +0.4 $M_\odot(\text{km s}^{-1})^2$ and -1.7 $M_\odot(\text{km s}^{-1})^2$ using the minimum separation distance.

Table 3. Space velocity of primary, space velocity of secondary, angle between the space velocity vectors (Nugent metric), relative space velocity, system escape velocity, mean physical distance separation, minimum distance separation, maximum distance separation and overlap in distances for STF 2486 AB.

WDS Identifier	Primary space velocity (km/s)	Secondary space velocity (km/s)	Angle between the space velocity vectors (degrees)	Relative space velocity (km/s)	System escape velocity using mean distance separation (km/s)	System escape velocity using minimum distance separation (km/s)	Mean separation distance (AU)	Minimum Separation distance (AU)	Maximum Separation distance (AU)	Overlap in distances (AU)
19121+4951 STF 2486 AB	88.6	89.1	2.1	3.2	3.0	4.3	371	176	4,335	3,672

4. Discussion

The mean distance separation of the primary and secondary of STF 2486 of 371 AU. The minimum separation distance is 176 AU and the maximum separation distance is 4,335 AU. The approximate upper bound for physical 3D separation of most binary systems is 2,500 AU (Nugent, 2026). It has been suggested that tightly bound binaries have separations of less than ~1,000 AU (Matson R, personal communication). The angle between the space velocity vectors of the components of STF 2486 AB is 2.1 degrees which indicates that the pair show common space motion. The relative space velocity and system escape velocity are similar. Moreover, the relative space velocity is less than the system escape velocity if the minimum separation distance is used in the calculation. The binding energy (E_{binding}) of STF 2486 AB is +0.4 which is considered by Letchford et al. 2022 to still be acceptable for a binary star system allowing for uncertainties in E_{binding} calculation. The binding energy becomes negative if the minimum separation distance is used in the calculation. The overall features are consistent with a binary star system.

Assuming a circular orbit and a semi-major axis of 186 AU and given the masses of the A and B components as 0.94 $M_{\odot}$ and 0.92 $M_{\odot}$, the orbital period (using Kepler's third law) is estimated to be 1,860 years which is comparable to Izmailov's estimate of 1,459 years. In contrast, the orbital period proposed by Romanenko et al, is 11,565 years (Romanenko et al. 2025).

5. Conclusion

Analysis using GAIA DR3 data and a current astrometric measure shows that WDS 19121+4951 STF 2486 AB exhibits features consistent with a binary star system.

Acknowledgements

I would like to thank Dr. Rachel Matson for providing the historical data and technical information required for the analysis of WDS 19121+4951 STF 2486 AB . I would also like to acknowledge the Boyce Research Initiatives and Education Foundation (https://boyce-astro.org/) and Pat Boyce for providing the technical support required to complete this paper.

This research has made use of the Washington Double Star Catalogue maintained at the U.S. Naval Observatory http://www.astro.gsu.edu/wds/ and the Las Cumbres Observatory Global Telescope Network (https://lco.global/).

This work has also made use of data from the European Space Agency (ESA) mission Gaia (https://www.cosmos.esa.int/gaia), processed by the Gaia Data Processing and Analysis Consortium (DAC, https://www.cosmos.esa.int/web/gaia/Dac/consortium).
Funding for the DAC has been provided by national institutions, in particular the institutions participating in the Gaia Multilateral Agreement.

6. References

Anton, R. (2017). Double Star Measurements at the Northern Sky with a 10 inch Newtonian in 2014 and 2015. Journal of Double Star Observations, 13(3). 288-298. Retrieved from: http://www.jdso.org/volume13/number3/July2017Issue.pdf

Bonifacio, B., Marchetti, C., Caputo, R., & Tock, K. (2020). Measurements of Neglected Double Stars. Journal of Double Star Observations, 16(5), 411-423. Retrieved from: http://www.jdso.org/volume16/number5/Bonifacio_411_423.pdf

Brabec, H., Bryant, K., Pedersen, A., & McCudden, P. (2025). CCD and Astrometric Eyepiece Measurements of WDS 19121+4951. Journal of Double Star Observations, 21(2), 156-166. Retrieved from: https://www.doublestarsjournal.org/index.php/jdso/article/view/16/19

Hale, A. (1994). Orbital Coplanarity in Solar-Type Binary Systems: Implications for Planetary System Formation and Detection. Astronomical Journal. 107(1), 306-332. Retrieved from: https://ui.adsabs.harvard.edu/scan/manifest/1994AJ....107..306H?art=true

Izmailov, I.S. (2019). The Orbits of 451 Wide Visual Double Stars. Ast. Lett. 45, 30. Retrieved from: https://journals.rcsi.science/1063-7737/article/view/191032

Letchford, R.R., White, G.L., & Brown, C.J. (2022). Orbital Elements of visual binary stars with very short arcs: With application to double stars from the 1829 southern double star Catalogue of James Dunlop. Astronomische Nachrichten. 343 (3), e210113. Retrieved from: https://doi.org/10.1002/asna.20210113

Matson, R.A., Williams, S.J., Hartkopf, W.I., & Mason, B.D. (2026). Sixth Catalog of Orbits of Visual Binary Stars. https://www.astro.gsu.edu/wds/orb6.html

Nugent, R.L. (2025). An Analysis of the Double Star Systems WDS 02109+1341 STF 224 and WDS 10013-2246 HDO 124AB in 3 Dimensions. Journal of Double Star Observations, 21(4). Retrieved from: https://doublestarsjournal.org/index.php/jdso/article/view/137/41

Nugent, R.L. (2026). Analysis of the Double Star System WDS 08230+0738 STF 1219. Journal of Double Star Observations, 22 (2), 101-108. Retrieved from: https://doublestarsjournal.org/index.php/jdso/article/view/172/74

Prusti, T., et al. (2016). The Gaia mission. A&A, 595, A1. Retrieved from: https://www.aanda.org/articles/aa/pdf/2016/11/aa29272-16.pdf

Romanenko, L.G., Kiyaeva, O.V., Izmailov, I.S., Shakht, N.A., and Gorshanov, D.L. (2025). The Pulkovo Catalog of the Orbits Obtained for Visual Binary and Multiple Stars by the Apparent Motion Parameters Method. Astronomy Reports, 2025, 69(5), 398–432. Retrieved from: https://izmccd.puldb.ru/vds9/AR398_69_05_2025.pdf

Schuhmacher, C. (2025). Mesures D'Étoiles Doubles visuelles avec un réfracteur de 152MM en Mai et Juin 2025. Visual double star measurements with a 6 inches refractor in May and June 2025 Etoiles Doubles 11, 2-5. Retrieved from: https://etoilesdoubles.org/revue/ED-2025-11/ED-2025-11-SCHUHMACHER.pdf

Struve, F.G.W.(1837). Stellarum duplicium et multiplicium Mensurae Micrometricae per magnum fraunhoferi tubum. (Dorpat, Academiae scientiarum caesareae petropolitaneifique). Retrieved from: http://www.brera.inaf.it/documenti/Struve/Mensurae-Micrometricae1824-1837.pdf

Vallenari, A., et al. (2023). Gaia Data Release 3. Summary of content and survey properties. A&A, 674, A1. Retrieved from: https://www.aanda.org/articles/aa/pdf/2023/06/aa43940-22.pdf